

Supplementary Information for

Small-angle neutron scattering differentiates molecular-level structural models of nanoparticle interfaces

Yujie Wu,^{†a} Xindi Liu,^{†a} Aurel Radulescu,^b Lionel Porcar,^c Anwen Krause-Heuer,^d Hanqiu Jiang,^{ef} Hua Yang,^{ef} Yubin Ke,^{ef} Tamim Darwish,^b Zhi Luo^{a}*

^a Department of Biomedical Engineering, Southern University of Science and Technology, Shenzhen 518055, China

^b Jülich Center for Neutron Science, JCNS at Heinz Maier-Leibnitz Zentrum, Forschungs-zentrum Jülich GmbH, Garching 85747, Germany

^c Institut Laue-Langevin, BP 156, F38042 Grenoble CEDEX 9, France

^d The National Deuteration Facility, Australian Nuclear Science and Technology Organisation, NSW 2232, Australia

^e Institute of High Energy Physics, Chinese Academy of Sciences (CAS), Beijing 100049, China

^f Spallation Neutron Source Science Center, Dongguan 523803, China

[†] *Authors contributed equally.*

AUTHOR INFORMATION

Corresponding author

*Email: luoz@sustech.edu.cn

This PDF file includes:

Materials and methods

Table S1. The SANS data were fitted using SASView software by a core-shell sphere model.

Table S2. The parameters that define the smearing condition in MONSA calculation.

Fig. S1. SANS curve of MUA-DDT gold nanoparticles.

Fig. S2. TEM images and ^1H NMR data of PET-OT gold nanoparticles.

Fig. S3. TEM images and ^1H NMR data of MUA-DDT gold nanoparticles.

Fig. S4. SANS data and MONSA models of MUS-OT gold nanoparticles and ideal morphology 3D models.

Fig. S5. TEM images and ^1H NMR data of MUS-OT gold nanoparticles.

Fig. S6. TEM images and ^1H NMR data of PET-DDT gold nanoparticles at different time points before and during the heating process.

Fig. S7. $P(r)$ functions of PET-DDT gold nanoparticles before thermo-treatment (0 h) and after conducting thermo-treatment for 24 h.

Reference

1 **Materials and Methods**

2 **Chemicals**

3 1-Octanethiol (dOT) and 1-dodecanethiol (dDDT) ligands were purchased from CDN Isotopes,
4 Inc. Deuterated 2-phenylethanethiol (dPET) and 11-mercaptoundecanoic acid (dMUA) ligands are
5 provided by the National Deuteration Facility at the Australian Nuclear Science and Technology
6 Organisation (ANSTO). The synthesis of the deuterated molecules is reported elsewhere¹. All
7 other chemicals were purchased from Sigma-Aldrich and used as received.

8 **Synthesis of mixed-ligand gold nanoparticles**

9 Homo-ligand protected nanoparticles synthesis followed the protocol reported by Stucky and co-
10 workers with solvents and feed ratios of ligand mixtures varied². First, homo-ligand alkanethiol
11 protected nanoparticles were synthesized as follows: 123 mg of triphenylphosphinegold (I)
12 chloride and 0.25 mmol of alkanethiol ligand (e.g., DDT, OT) were dissolved in the 20 mL of
13 chloroform and 20 mL of toluene mixtures. The solution was heated to 70 °C for 10 min before
14 217 mg of borane t-butylamine complex was added under rapid stirring. The reaction proceeded
15 for 1 h before cooling down to room temperature. An excess amount of methanol (50 mL) was
16 added to quench the reaction and precipitate the nanoparticles. Black pellets of gold nanoparticles
17 were first collected by centrifugation (Thermo Fisher Sorvall ST 16R) at 4000 rpm and then
18 redispersed in 40 mL of antisolvent, acetone, using a vortex mixer (IKA) at full speed. The vortex
19 mixing was performed for more than 3 min to make sure that the pellets were broken into small
20 pieces. The suspension was then precipitated using centrifugation at 4000 rpm. The antisolvent
21 purification step was then repeated 2 times using acetone and 2 times using methanol. The final
22 solid product was dried in vacuum overnight. A typical synthesis yielded 40 mg of gold
23 nanoparticles, corresponding to 90% conversion in terms of the gold element.

24 The ligand exchange reaction was performed using the following protocol: 30 mg of DDT or OT
25 protected gold nanoparticles were dissolved in 15 mL of chloroform. Different amounts of
26 exchanging ligand molecules were added to the solution under stirring at room temperature.
27 Specifically, for MUS-OT nanoparticles, 3 mg of MUS molecules were used. The reaction was
28 quenched at 12 h. For MUA-DDT nanoparticles, 3 mg of MUA ligand was added into the
29 chloroform solution of gold nanoparticles, and the reaction proceeded for 12 h in order to achieve

30 a ligand ratio of MUA: DDT around 2: 1. 20 mL of washing solvent (hexane for MUA-DDT and
31 MUS-OT nanoparticles, methanol for PET-OT and PET-DDT nanoparticles) was added in order
32 to fully precipitate the nanoparticles. The black precipitate was collected using centrifugation at
33 4000 rpm. The nanoparticles were then redispersed using the same solvent to form suspensions
34 with the help of a vortex mixer before centrifugation at 4000 rpm. The washing procedure was
35 repeated 3 times before the black pellets were dried under vacuum overnight.

36 **NMR**

37 ¹H NMR spectra were taken using a Bruker 400 MHz spectrometer using deuterated chloroform
38 as the solvent for PET-DDT and PET-OT nanoparticles, and D₂O as the solvent for MUA-DDT
39 and MUS-OT nanoparticles. To determine the ligand shell composition, the gold core was etched
40 using iodine before ¹H NMR measurement. Briefly, a stock iodine solution with a concentration
41 of 20 mg/mL was first prepared. Then 0.6 mL of the stock solution was added to 5 mg of gold
42 nanoparticles in a glass vial. The vial was then capped, sealed with parafilm, and sonicated for 10
43 min. The supernatant was then taken for ¹H NMR measurement.

44 **TEM**

45 TEM images were taken using an FEI Tecnai Osiris instrument at an accelerating voltage of 120
46 kV. The nanoparticle samples were prepared by drop-casting 2 μL of the above-mentioned ethanol
47 solution (0.1 mg/mL) onto the carbon-coated-copper 400 mesh grid following by drying under
48 ambient condition. The size and polydispersity of the nanoparticles were characterized by TEM.
49 Image analysis was based on statistics of more than 500 nanoparticles by the software Image J.

50 **SANS**

51 SANS measurements were mainly conducted on KWS-2 at Jülich Center for Neutron Science. The
52 SANS of MUS-OT nanoparticles were performed on D22 at Institut Laue-Langevin
53 (<http://doi.ill.fr/10.5291/ILL-DATA.8-03-876>). Measurements were performed at 20 °C, using
54 1.4 m sample-to-detector distance, at 2.8 Å wavelength with a collimation setup of 5.6 m and a q
55 range from 0.04 Å⁻¹ to 0.8 Å⁻¹. The sample concentration was approximately 10 mg/ml
56 corresponding to a volume fraction of gold nanoparticles solution of around 0.1%. The two-
57 dimensional scattering data were processed and reduced using Grasp software including radial
58 averaging, background subtraction, empty cell and transmission correction, and normalization to

59 an absolute scale. The time-of-flight SANS data of MUA-DDT gold nanoparticles (Fig. S1) were
60 collected at the Chinese Spallation Neutron Source. Measurements were carried out at room
61 temperature, with sample-to-detector distance set to 4 m and the sample aperture diameter set to 6
62 mm. A neutrons wavelength band of 1.2 Å to 9.8 Å was utilized, corresponding to a q-range of
63 0.005 Å⁻¹ to 0.69 Å⁻¹. The sample concentration was approximately 10 mg/ml. The data acquisition
64 time was 2 h for each sample. The two-dimensional scattering data were processed and reduced
65 using QtiKWS software including radial averaging, background subtraction, empty cell and
66 transmission correction, and normalization to an absolute scale.

67 **Data analysis**

68 For ab initio fitting and 3D model reconstruction from the SANS data, the MONSA program in
69 ATSAS software was used. In brief, a spherical search volume composed of close packed small
70 beads with a 2 Å radius was generated according to the D_{\max} value in the P(r) function. As the core
71 radius is 28 Å, the beads within the central 24 Å radius were fixed to gold in order to reduce the
72 calculation time and act as physical constraints. Between a radius of 30 Å and a radius of 38 Å,
73 the bead assignments were limited to the different ligands or solvent, while all other beads were
74 free to be assigned to all four possible components. SLD pattern was generated by SASView using
75 the onion model to fit the SANS curve of MUA-dDDT nanoparticles with TEA. The simulated
76 annealing algorithm implemented in MONSA then searches for the best bead assignments, i.e., 3D
77 model that fits simultaneously all the SANS curves and minimizes the overall discrepancy between
78 the experimental data and fits based on the theoretical spectra of the multiphase bead model. The
79 master file, control file and PDB-like files have the following contents or formats (PDB):

80 Control file:

```
81 'NP.res' 2
82 'NP.fit'
83 NP test 10%
84 64
85 'NP-CDC13.dat' 1.51 -3.434 1.36 0.00 1.000 0. 1.00
86
87 'NP-tol.dat' -0.99 -5.94 -1.14 0.00 1.000 0. 1.00
88
```

89

90 Master file:

91 Master file for PET-DDT NPs neutron 3 phases

92 14.1e3 25.8e3 7.32e3 0.0 ! Desired Volumes

93 -1.0 -1.0 -1.00 0.0 ! Desired Rgs

94 1 1 1 0 ! Connectivity

95 'NP.con' -1 ! Control file and nRg

96

97 PDB-like file (format only, not all beads coordinates are listed):

98 Created by DAM2DAM : Mon Nov 10

99 -----

100 Coordinates taken from : sph34-43.pdb

101 Number of atoms read : 7376

102 Center of the reference DAM : 0.0000 0.0000 0.0000

103 Maximum radius : 42.80

104 Atomic radius : 2.000

105 -----

106 Phases taken from : sph26.pdb

107 Number of atoms read : 1638

108 Center of the DAM to regrid : 0.0000 0.0000 -0.0000

109 Maximum radius : 25.77

110 Number of phases : 3

111 Atomic radius : 2.000

112 -----

113 Offset to closest reference atom : 2.500

114 -----

115 ATOM 1 H ASP 1 -4.000 -4.000 -42.426 1.00 20.00 0 1 202

116 ATOM 2 H ASP 1 -4.000 0.000 -42.426 1.00 20.00 0 1 202

117 ATOM 3 H ASP 1 -4.000 4.000 -42.426 1.00 20.00 0 1 202

118 ATOM 4 H ASP 1 0.000 -4.000 -42.426 1.00 20.00 0 1 202

119 ATOM 5 H ASP 1 0.000 0.000 -42.426 1.00 20.00 0 1 202

120 Etc...

122 **Table S1.**

Parameter	Value	Units
Scale	1	
Background	0	cm ⁻¹
Radius	50	Å
Thickness	12	Å
Sld_core	4.67	10 ⁻⁶ / Å ²
Sld_shell	2.0	10 ⁻⁶ / Å ²
Sld_solvent	3.0	10 ⁻⁶ / Å ²
Q range	0.04- 0.221	Å ⁻¹
Custom pinhole smearing	0, 0.1, or 0.2	
Polydisperse parameters	0, 0.1, or 0.2	

123 The SANS data were fitted using SASView software by a core-shell sphere model. Calculated
124 SANS curves with a core size polydispersity of 0%, 10% and 20%. Calculated SANS curves of
125 the same nanoparticle under different pinhole smearing conditions, i.e., 0%, 10%, 20%.

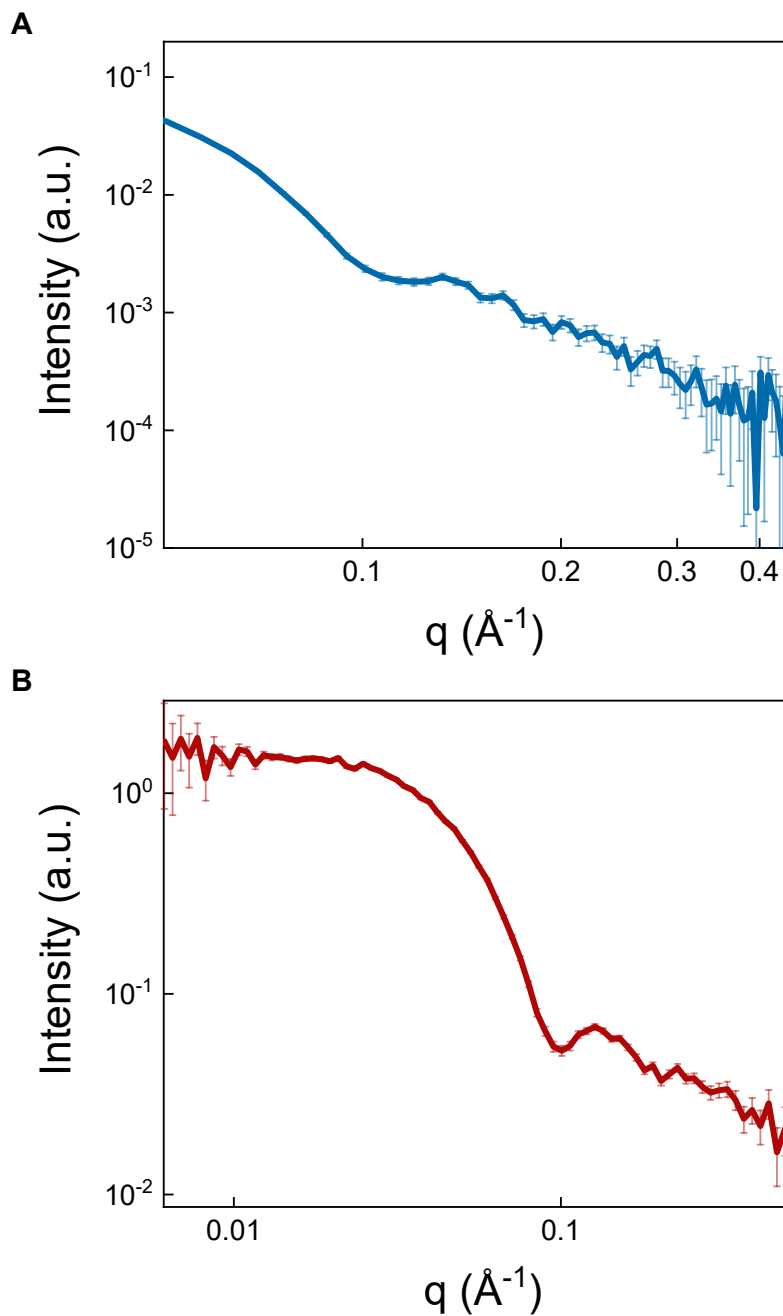
126

127 **Table S2.**

Effective collimation slit diameter in cm	3.00
Effective sample diameter in cm	1.46
Collimation distance in cm	600
Sample-detector distance in cm	160
λ in Å	5.00
$\delta(\lambda)/\lambda$	0.10
Pixel size in cm	0.75
Averaging error	0

128 The parameters that define the smearing condition in MONSA calculation.

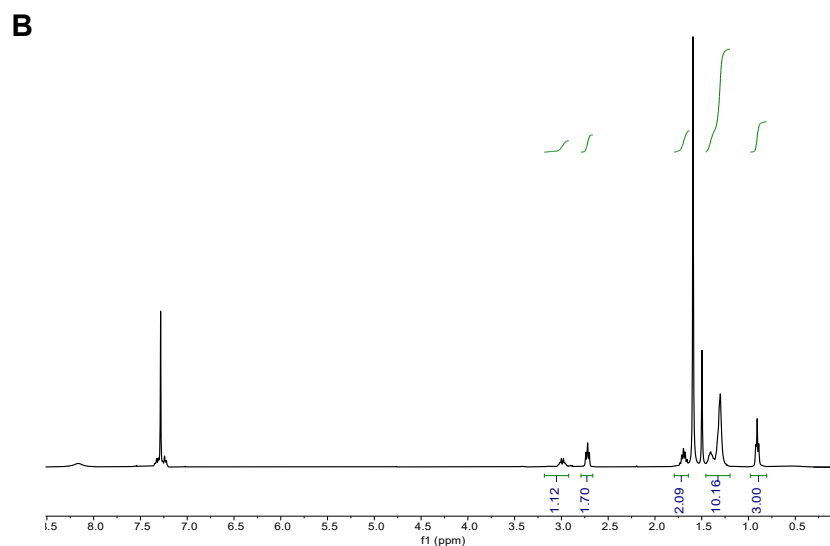
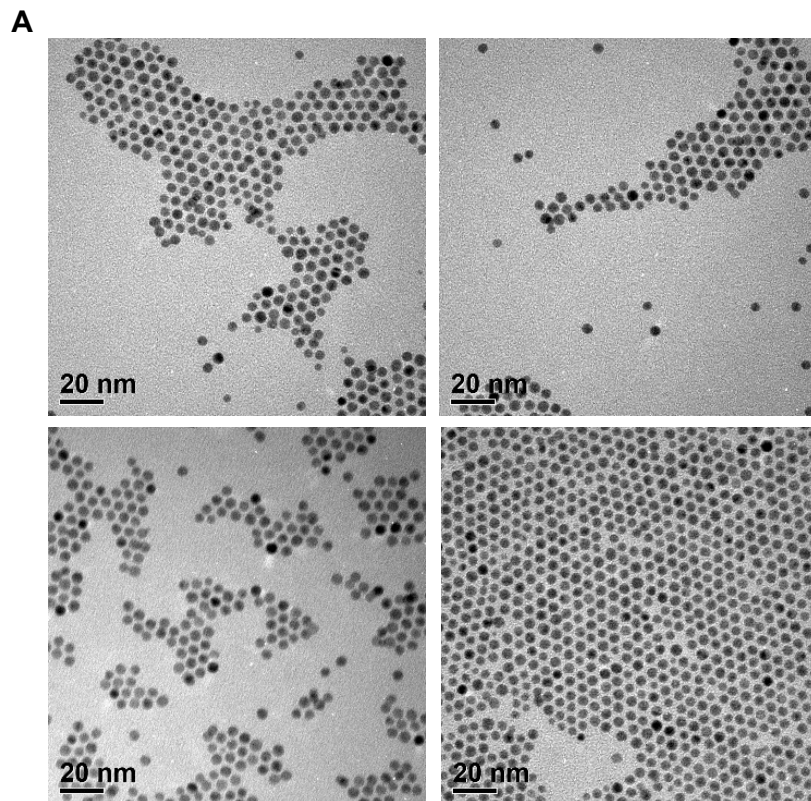
129



130

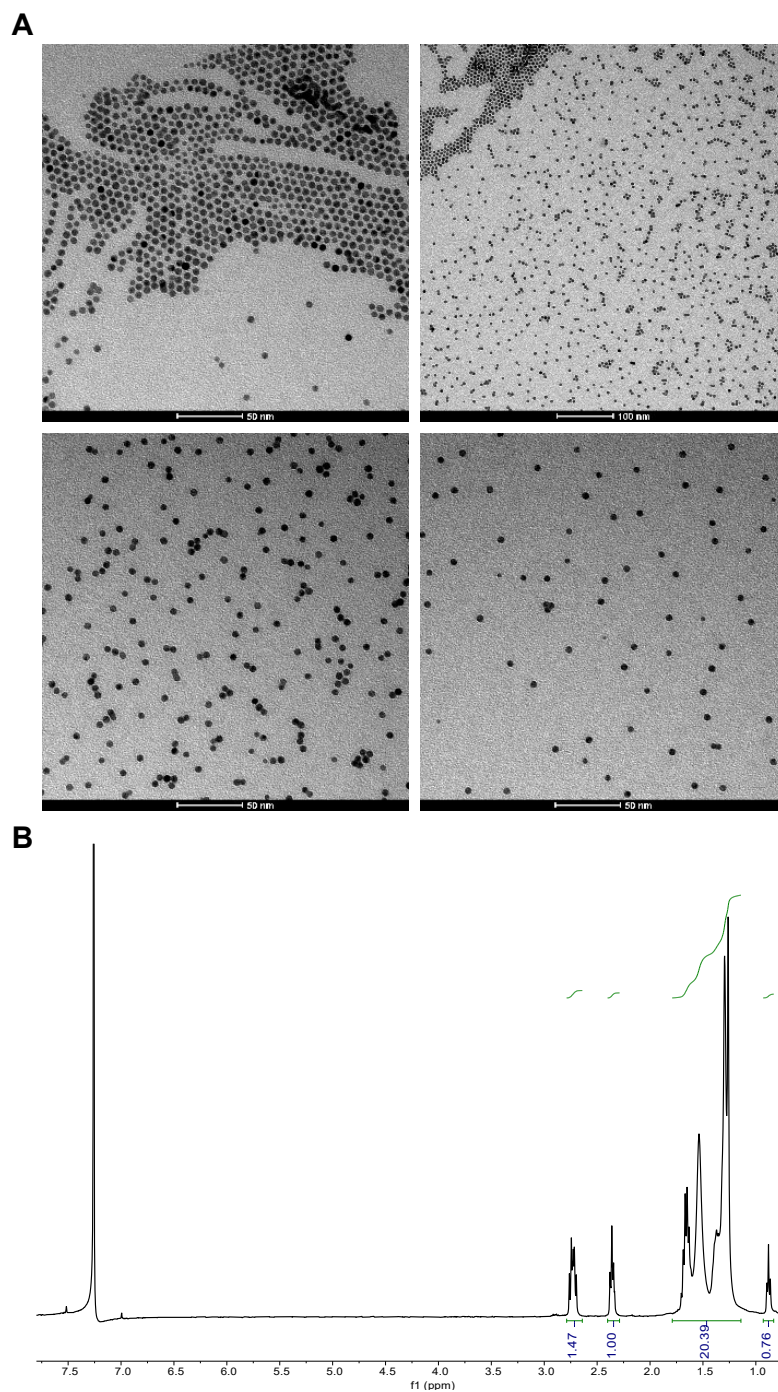
131 **Fig. S1. SANS curve of MUA-DDT gold nanoparticles.** (A) MUA-DDT gold nanoparticles with
132 35% polydispersity. (B) SANS data of MUA-DDT gold nanoparticles achieved by time-of-flight
133 instrument on spallation sources.

134



135

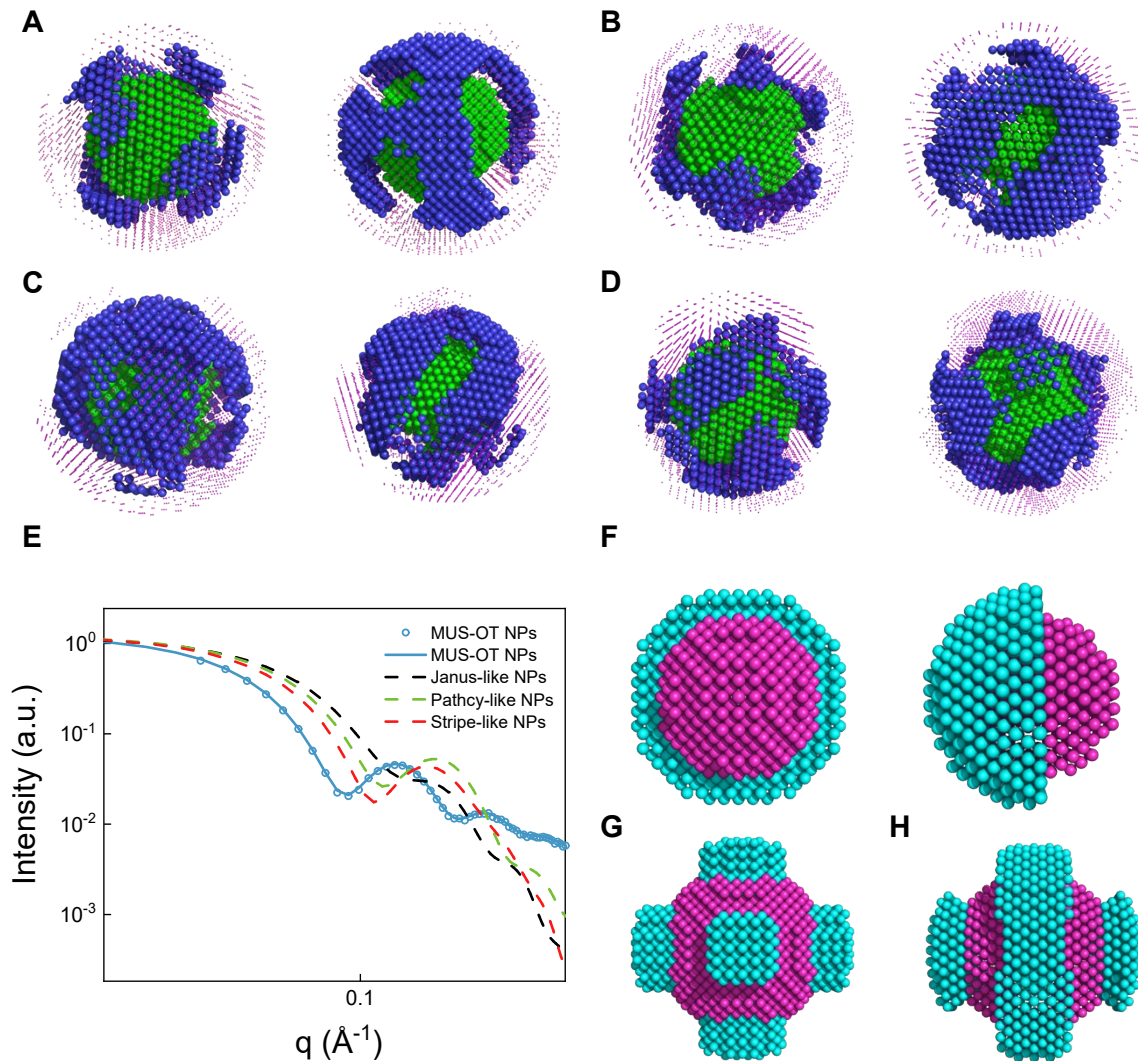
136 **Fig. S2. TEM images and ^1H NMR data of PET-OT gold nanoparticles.** (A) TEM images of
 137 4.7 ± 0.4 nm PET-OT gold nanoparticles. The averaged sizes are calculated based on statistics of
 138 more than 500 counts. (B) ^1H NMR spectrum of PET-OT gold nanoparticles, the calculated ligand
 139 ratio is PET: OT = 42.4%: 57.6%.



140

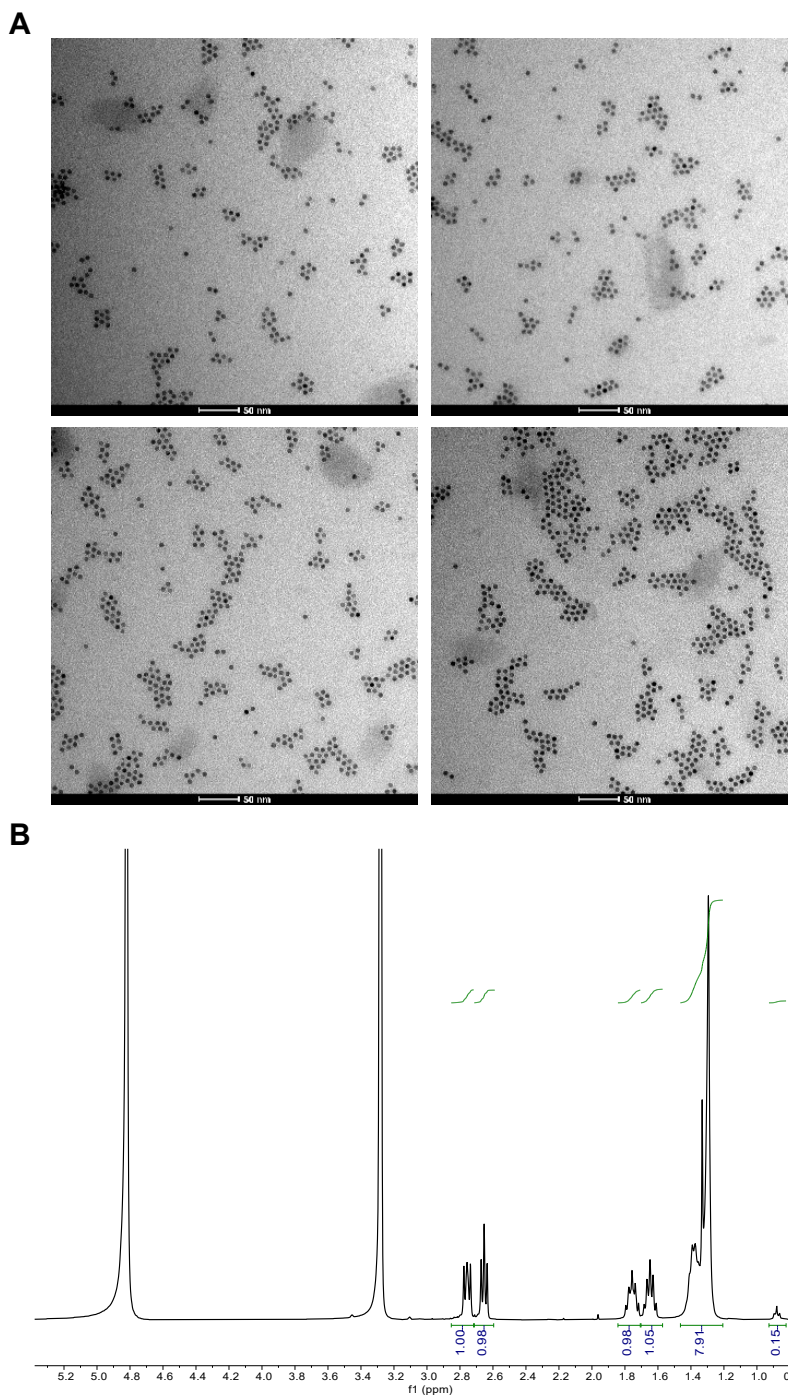
141 **Fig. S3. TEM images and ^1H NMR data of MUA-DDT gold nanoparticles.** (A) 5.2 ± 0.6 nm
 142 MUA-DDT gold nanoparticles. The averaged sizes are calculated based on statistics of more than
 143 500 counts. (B) ^1H NMR spectrum of PET-OT gold nanoparticles, the calculated ligand ratio is
 144 MUA: DDT = 68.0%: 32.0%.

145



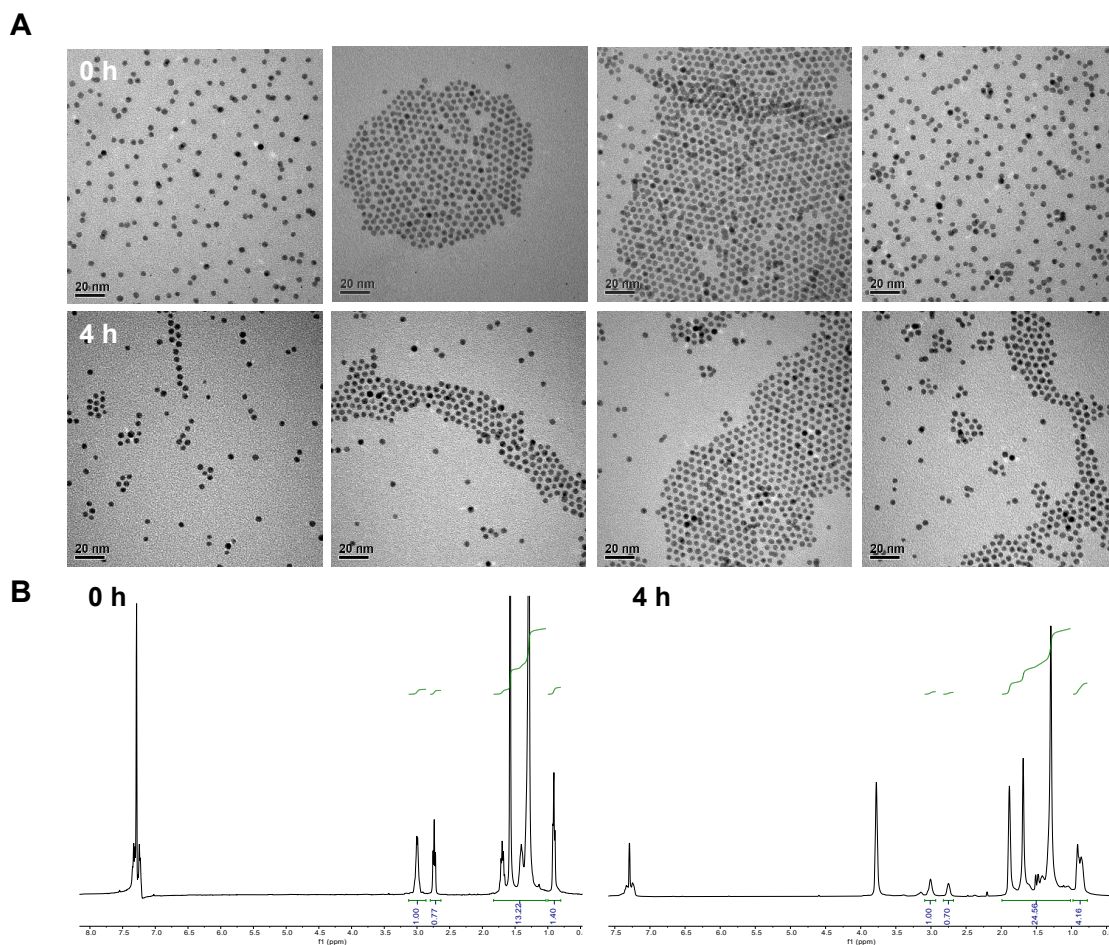
146

147 **Fig. S4. SANS data and MONSA models of MUS-OT gold nanoparticles and ideal**
 148 **morphology 3D models.** (A-D) MONSA models fitting from different initial random
 149 configurations of MUS-OT gold nanoparticles. (E) SANS curves of MUS-OT gold nanoparticles
 150 (blue line), Janus-like nanoparticles (black dotted line), patchy-like nanoparticles (green dotted
 151 line) and stripe-like nanoparticles (red dotted line). (F) 3D model of the Janus-like nanoparticles.
 152 (G) 3D model of the patchy-like nanoparticles. (H) 3D model of the stripe-like nanoparticles.
 153 Comparison with theoretical scattering patterns of the ideal Janus, patchy and stripe type of
 154 morphology clearly deviates from the experimental MUS-OT gold nanoparticles curve.



155

156 **Fig. S5. TEM images and ^1H NMR data of MUS-OT gold nanoparticles.** (A) 5.2 ± 0.4 nm
 157 MUS-OT gold nanoparticles. The averaged sizes are calculated based on statistics of more than
 158 500 counts. (B) ^1H NMR spectrum of MUS-OT gold nanoparticles, the calculated ligand ratio is
 159 MUS: OT = 90.9%: 9.1%.



160

161 **Fig. S6. TEM images and ^1H NMR data of PET-DDT gold nanoparticles at different time**
 162 **points before and during the heating process. (A) TEM images of PET-DDT gold nanoparticles**
 163 **before (0 h) and thermo-treatment after 4 h. TEM images of nanoparticles before and after thermo-**
 164 **treatment, showing that the core sizes of the nanoparticles are not affected by the thermo-**
 165 **(B) ^1H NMR spectra of PET-DDT gold nanoparticles before thermo-treatment (0 h) and**
 166 **conducting thermo-treatment after 4 h showing no detectable change of ligand density and ratio.**

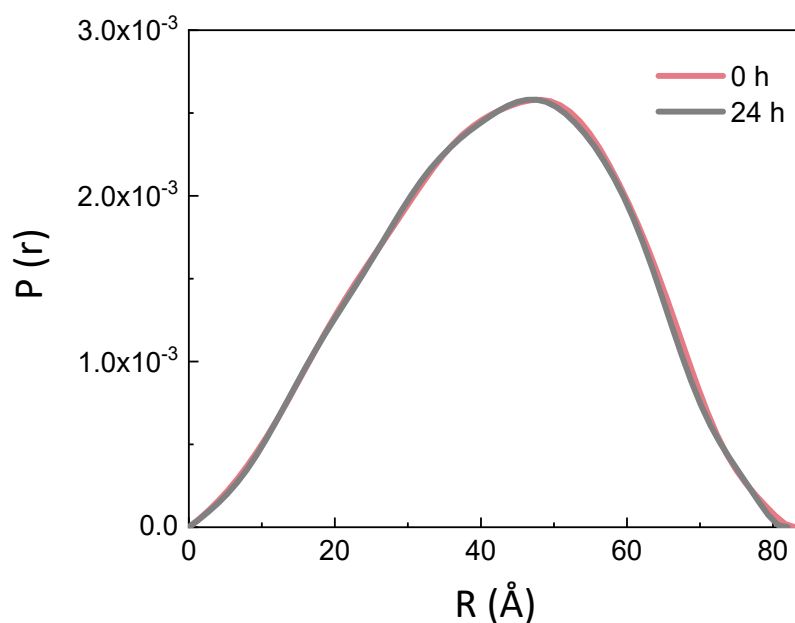


Fig. S7. $P(r)$ functions of PET-DDT gold nanoparticles before thermo-treatment (0 h) and after conducting thermo-treatment for 24 h. The D_{\max} and the shape of the curve show there are no obvious shape and size change of PET-DDT nanoparticles after the thermo-treatment.

Reference

1. Z. Luo, D. Marson, Q. K. Ong, A. Lojudice, J. Kohlbrecher, A. Radulescu, A. Krause-Heuer, T. Darwish, S. Balog, R. Buonsanti, D. I. Svergun, P. Posocco, F. Stellacci. *Nat Commun.*, 2018, **9**, 1343.
2. N. Zheng, J. Fan, G. D. Stucky. *J. Am. Chem. Soc.*, 2006, **128**, 6550–6551.